

Article

# IMMIGRATE: A Margin-based Feature Selection Method with Interaction Terms

Ruzhang Zhao<sup>1</sup>, Pengyu Hong<sup>2,\*</sup> and Jun S. Liu<sup>3,\*</sup><sup>1</sup> Department of Biostatistics, Bloomberg School of Public Health, Johns Hopkins University; rzhao@jhu.edu<sup>2</sup> Department of Computer Science, Brandeis University; hongpeng@brandeis.edu<sup>3</sup> Department of Statistics, Harvard University; jliu@stat.harvard.edu

\* Correspondence: hongpeng@brandeis.edu, Tel.: +1-781-736-2729; jliu@stat.harvard.edu, Tel.: +1-617-495-1600

Version February 19, 2020 submitted to Entropy

**Abstract:** Traditional hypothesis-margin researches focus on obtaining large margins and feature selection. In this work, we show that the robustness of margins is also critical and can be measured using entropy. In addition, our approach provides clear mathematical formulations and explanations to uncover feature interactions, which is often lack in large hypothesis-margin based approaches. We design an algorithm, termed IMMIGRATE, for training the weights associated with the interaction terms. IMMIGRATE simultaneously utilizes both local and global information and can be used as a base learner in Boosting. We evaluate IMMIGRATE in a wide range of tasks, in which it demonstrates exceptional robustness and achieves the state-of-the-art results with high interpretability.

**Keywords:** hypothesis-margin; feature selection; entropy; IMMIGRATE

## 1. Introduction

Feature selection is one of the most fundamental problems in machine learning and pattern recognition [1]. The Relief algorithm by Kira and Rendell [2] is one of the most successful feature selection algorithms. It can be interpreted as an online learning algorithm that solves a convex optimization problem with a hypothesis-margin-based cost function. Instead of deploying exhaustive or heuristic combinatorial searches, Relief decomposes a complex, global and nonlinear classification task into a simple and local one. Following the large hypothesis-margin principle for classification, Relief calculates the weights of features, which can be used for feature selection. The hypothesis-margin of an instance  $x$  with respect to (w.r.t.) a set of samples  $\mathcal{P}$  is later **formerly** defined in Gilad-Bachrach *et al.* [3] as  $\frac{1}{2}(\|\vec{x} - \text{NM}(\vec{x})\| - \|\vec{x} - \text{NH}(\vec{x})\|)$ , where  $\text{NH}(\vec{x})$  and  $\text{NM}(\vec{x})$  denote the nearest samples to  $\vec{x}$  in  $\mathcal{P}$  with the same and different labels, respectively. The large hypothesis-margin principle has motivated several successful extensions of the Relief algorithm. For example, ReliefF [4] uses multiple nearest neighbors. Simba [3] recalculates the nearest neighbors every time the feature weights are updated. Yang *et al.* [5] consider global information to improve Simba. I-RELIEF [6] identifies the nearest hits and misses in a probabilistic manner, which forms a variation of hypothesis-margin. LFE [7] extends Relief from feature selection to feature extraction using local information. IM4E is proposed by Bei and Hong [8] to balance margin-quantity maximization and margin-quality maximization. Both approaches in Sun and Wu [7], Bei and Hong [8] use a variation of hypothesis-margin proposed in Sun and Li [6].

The Relief-based algorithms indirectly consider feature interactions by normalizing the feature weights [9], which, however, cannot directly reflect the natural effects of associations and hence results in poor interpretability on the effects of feature interactions. For example, Relief and many of its extensions cannot tell whether a high weight of a certain feature is caused by its linear effect or its

33 interaction with other features [9]. Similarly, these methods cannot clearly reveal the influence of  
 34 interaction terms on classification. In particular, the degree of such influence cannot be measured.

35 To this end, we propose the *Iterative Max-Min entropy marGin-maximization with inteRAction*  
 36 *TErms* algorithm (IMMIGRATE, henceforth). IMMIGRATE directly measures the influence of feature  
 37 interactions and delivers the following novelties. First, when defining our hypothesis-margin, we  
 38 introduce a new trainable quadratic-Manhattan measurement to capture interaction terms, which  
 39 interprets interaction importance directly. Second, we take advantage of the margin stability by  
 40 measuring the underlying entropy based on the distributions of instances. Third, we derive an  
 41 iterative optimization algorithm to efficiently minimize the cost function. Fourth, we design a novel  
 42 classification method that utilizes the learned quadratic-Manhattan measurement to predict the class  
 43 of a new instance. Fifth, we design a more powerful approach (i.e., Boosted IMMIGRATE) by using  
 44 IMMIGRATE as the base learner of Boosting [10]. Sixth, to make IMMIGRATE efficient for analyzing  
 45 high-dimensional datasets, we take advantage of IM4E [8] to provide an effective initialization.

46 The rest of the paper is organized as follows. Section 2 explains the foundation of the Relief  
 47 algorithm. The IMMIGRATE algorithm is explained in Section 3. Section 4 summarizes and discusses  
 48 the experiments on different datasets. Experimental results show that our approach achieves the  
 49 state-of-the-art results. Boosted IMMIGRATE outperforms other Boosting classifiers significantly. The  
 50 computation time of IMMIGRATE is comparable to other popular feature selection methods that  
 51 consider interaction terms. The paper is concluded and discussed in Section 5 including comparisons  
 52 with related works.

## 53 2. Review: the Relief Algorithm

We first explain a few notations used in the rest of the paper:  $\vec{x}_i$  as the  $i$ -th instance in the training  
 set  $\mathcal{P}$ ;  $y_i$  as the class label of  $\vec{x}_i$ ;  $N$  as the size of  $\mathcal{P}$ ;  $A$  as the number of features (i.e. attributes);  $\vec{w}$  as the  
 feature weight vector; and  $|\vec{x}_i|$  as a vector where absolute value operation is element-wise. Relief [2]  
 iteratively calculates the feature weights in  $\vec{w}$  (Algorithm 1). The higher a feature weight is, the more  
 relevant the corresponding feature is. After the calculation of feature weights, a threshold is chosen to  
 select relevant features. Relief can be viewed as a convex optimization problem that minimizes the  
 cost function:

$$C = \sum_{n=1}^M (\vec{w}^T |\vec{x}_n - \text{NH}(\vec{x}_n)| - \vec{w}^T |\vec{x}_n - \text{NM}(\vec{x}_n)|), \quad (2.1)$$

subject to :  $\vec{w} \geq 0, \|\vec{w}\|_2^2 = 1,$

54 where  $M (\ll N)$  is a user defined number of randomly chosen training samples,  $\text{NH}(\vec{x})$  is the nearest  
 55 "hit" (from the same class) of  $\vec{x}$ ;  $\text{NM}(\vec{x})$  is the nearest "miss" (from a different class) of  $\vec{x}$ ; and  $\vec{w}^T |\vec{x}_n -$   
 56  $\text{NH}(\vec{x}_n)|$  is the weighted Manhattan distance. Denote  $\vec{u} = \sum_{n=1}^M (|\vec{x}_n - \text{NH}(\vec{x}_n)| - |\vec{x}_n - \text{NM}(\vec{x}_n)|)$ .  
 57 Minimizing the cost function of Relief 2.1 can be solved using the Lagrange multiplier method and the  
 58 Karush-Kuhn-Tucker conditions [11] to get a close form solution:  $\vec{w} = (-\vec{u})^+ / \|(-\vec{u})^+\|_2$ , where  $(\vec{a})^+$   
 59 truncates the negative elements to 0. This solution to the original Relief algorithm is important for  
 60 understanding the Relief-based algorithms.

**Algorithm 1** The Original Relief Algorithm

$N$ : the number of training instances.

$A$ : the number of features(i.e. attributes).

$M$ : the number of randomly chosen training samples to update feature weight  $\vec{w}$ .

**Input:** a training dataset  $\{z_n = (\vec{x}_n, y_n)\}_{n=1, \dots, N}$ .

**Initialization:** Initialize all feature weights to 0:  $\vec{w} = 0$ .

**for**  $i = 1$  **to**  $M$  **do**

Randomly select an instance  $\vec{x}_i$  and find its  $\text{NH}(\vec{x}_i)$  and  $\text{NM}(\vec{x}_i)$ .

Update the feature weights by  $\vec{w} = \vec{w} - (\vec{x}_i - \text{NH}(\vec{x}_i))^2 / M + (\vec{x}_i - \text{NM}(\vec{x}_i))^2 / M$ ,

where the square operation is element-wise.

**Return:**  $\vec{w}$ .

### 61 3. IMMIGRATE Algorithm

62 IMMIGRATE stands for **I**terative **M**ax-**M**in entropy mar**G**in-maximization with inter**A**ction  
 63 **T**erms algorithm (IMMIGRATE, henceforth). Without loss of generality, we establish the IMMIGRATE  
 64 algorithm in a general binary classification setting. This formulation can be easily extended to  
 65 handle multiple class classification problems. Our implementation of IMMIGRATE is applicable to  
 66 multiple classification tasks. Let the whole data set be  $\mathcal{P} = \{z_n | z_n = (\vec{x}_n, y_n), \vec{x}_n \in \mathbb{R}^A, y_n = \pm 1\}_{n=1}^N$ ;  
 67 the hit index set of  $\vec{x}_n$  be  $\mathcal{H}_n = \{j | z_j \in \mathcal{P}, y_j = y_n \& j \neq n\}$ , and the miss index set of  $\vec{x}_n$  be  
 68  $\mathcal{M}_n = \{j | z_j \in \mathcal{P}, y_j \neq y_n\}$ .

#### 69 3.1. Hypothesis-Margin

Given a distance  $d(\vec{x}_i, \vec{x}_j)$  between two instances  $\vec{x}_i$  and  $\vec{x}_j$ , a hypothesis-margin [3] is defined as  
 $\rho_{n,h,m} = d(\vec{x}_n, \vec{x}_m) - d(\vec{x}_n, \vec{x}_h)$ , where  $\vec{x}_h, h \in \mathcal{H}_n$  and  $\vec{x}_m, m \in \mathcal{M}_n$  represent the nearest hit and nearest  
 miss for instance  $\vec{x}_n$ , respectively. We adopt the probabilistic hypothesis-margin defined by Sun and Li  
 [6] as

$$\rho_n = \sum_{m \in \mathcal{M}_n} \beta_{n,m} d(\vec{x}_n, \vec{x}_m) - \sum_{h \in \mathcal{H}_n} \alpha_{n,h} d(\vec{x}_n, \vec{x}_h), \quad (3.2)$$

70 where  $\alpha_{n,h} \geq 0$ ,  $\beta_{n,m} \geq 0$ ,  $\sum_{h \in \mathcal{H}_n} \alpha_{n,h} = 1$ ,  $\sum_{m \in \mathcal{M}_n} \beta_{n,m} = 1$ , for  $\forall n \in \{1, \dots, N\}$ . As in the above  
 71 design, the hidden random variable  $\alpha_{n,h}$  represents the probability that  $\vec{x}_h$  is the nearest hit of instance  
 72  $\vec{x}_n$ , while  $\beta_{n,m}$  indicates the probability that  $\vec{x}_m$  is the nearest miss of instance  $\vec{x}_n$ .

#### 73 3.2. Entropy to Measure Hypothesis-Margin Stability

74 Here, we consider how the distributions of the hits and misses contribute to the stability of the  
 75 hypothesis-margin(hypothesis-margin quality). That is to say, how the distributions of instances with  
 76 the same or different labels w.r.t. target instance can get more stable margins.

77 The probabilities  $\{\alpha_{n,h}\}$  and  $\{\beta_{n,m}\}$  in Eq. 3.2 represent the distributions of hits and misses.  
 78 The stability of an instance  $\vec{x}_n$ 's hypothesis-margin can be defined using its hit probabilities  $\{\alpha_{n,h}\}$   
 79 and miss probabilities  $\{\beta_{n,m}\}$ . Let's check the hit entropy and miss entropy, which are defined as  
 80  $E_{hit}(\vec{x}_n) = -\sum_{h \in \mathcal{H}_n} \alpha_{n,h} \log \alpha_{n,h}$  and  $E_{miss}(\vec{x}_n) = -\sum_{m \in \mathcal{M}_n} \beta_{n,m} \log \beta_{n,m}$ , respectively. The following  
 81 two scenarios help to explain the intuition of using the hit entropy and miss entropy. Scenario  
 82 A(stability): all neighbors are distributed evenly around the target instance; scenario B(instability):  
 83 the neighbor distribution is highly uneven. An extreme example for scenario B is that one instance is  
 84 quite close to the target and the rest are quite far away from the target. An easy experiment to test  
 85 the stability of the distributions of hits and misses is to discard one instance from the system and to  
 86 check the change degree of hypothesis-margin. In scenario A, if the true nearest hit is discarded, the  
 87 margin changes slightly since there are many other hits evenly distributed around target. However,  
 88 in scenario B, the disappearance of the true nearest miss can increase the margin significantly. In

89 details, the disappearance of the true nearest miss makes the other misses have larger probabilities to  
 90 be the nearest miss ( $\{\beta_{n,m}\}$ ), which results in the increase of margin in Eq. 3.2. However, if scenario B  
 91 works for hits, the margin will decrease accordingly when the true nearest hit disappears. Similarly, if  
 92 scenario A works for misses, the even distribution will not contribute to the margin. In conclusion,  
 93 hits prefer scenario A(stability) and misses scenario B(instability).

94 Since scenario A and B are corresponding to hit and low entropies, respectively, the margin can  
 95 benefit from a large hit entropy  $E_{hit}$  (e.g., scenario A) and a low miss entropy  $E_{miss}$  (e.g., scenario B).  
 96 We can set up a framework to maximize the hit entropy and minimize the miss entropy, which is  
 97 equivalent to make the hypothesis-margin in Eq. 3.2 the most stable. We call the level of stability of  
 98 hypothesis-margin as hypothesis-margin quality. And Bei and Hong [8] use the term max-min entropy  
 99 principle to describe the process that we maximize the hit entropy and minimize the loss entropy to  
 100 maximize the hypothesis-margin quality. Actually, the process of maximizing stable hypothesis-margin  
 101 is an extension of the large hypothesis-margin principle.

### 102 3.3. Quadratic-Manhattan Measurement

103 We extend the margin in Eq. 3.2 by using a new quadratic-Manhattan measurement defined in  
 104 Eq. 3.3:

$$q(\vec{x}_i, \vec{x}_j) = |\vec{x}_i - \vec{x}_j|^T \mathbf{W} |\vec{x}_i - \vec{x}_j|, \quad (3.3)$$

105 where  $\mathbf{W}$  is a non-negative symmetric matrix (element-wise non-negative) and its Frobenius norm  
 106  $\|\mathbf{W}\|_F = 1$ . The quadratic-Manhattan measurement is a natural extension of the weight vector. The  
 107 off-diagonal elements in  $\mathbf{W}$  capture the feature interactions and the diagonal elements in  $\mathbf{W}$  capture  
 108 the features. Here, we explain the motivation why quadratic-Manhattan measurement can capture  
 109 the influence of interactions. For example,  $w_{a,b}$  ( $a \neq b$ ), the element in the  $a$ -th row and  $b$ -th column  
 110 of  $\mathbf{W}$ , reflects the influence of the interactions between two features  $a$  and  $b$ . In details, according  
 111 to the extension of quadratic form,  $w_{a,b}$  ( $a \neq b$ ) is the coefficient for the combination of the  $a$ -th and  
 112  $b$ -th elements in vector  $|\vec{x}_i - \vec{x}_j|$ . The quadratic-Manhattan measurement is a natural extension of  
 113 the weighted Manhattan distance in Eq. 2.1. In Relief-based algorithms, the motivation of weighted  
 114 Manhattan distance Eq. 2.1 can be equivalently captured by the feature weight update equation in  
 115 Algorithm 1. Similarly,  $w_{a,b}$  can be updated using the combination of the  $a$ -th and  $b$ -th features based  
 116 on a randomly given instance, which is a straightforward way to understand the process of capturing  
 117 interactions.

We define our new hypothesis-margin using the quadratic-Manhattan measurement as

$$\sum_{m \in \mathcal{M}_n} \beta_{n,m} q(\vec{x}_n, \vec{x}_m) - \sum_{h \in \mathcal{H}_n} \alpha_{n,h} q(\vec{x}_n, \vec{x}_h). \quad (3.4)$$

### 118 3.4. IMMIGRATE

119 We design the following cost function Eq. 3.5 to maximize our new hypothesis-margin (quantity)  
 120 and the hypothesis-margin quality simultaneously:

$$\begin{aligned} C = & \sum_{n=1}^N \left( \sum_{h \in \mathcal{H}_n} \alpha_{n,h} |\vec{x}_n - \vec{x}_h|^T \mathbf{W} |\vec{x}_n - \vec{x}_h| - \sum_{m \in \mathcal{M}_n} \beta_{n,m} |\vec{x}_n - \vec{x}_m|^T \mathbf{W} |\vec{x}_n - \vec{x}_m| \right) \\ & + \sigma \sum_{n=1}^N [E_{miss}(z_n) - E_{hit}(z_n)], \end{aligned} \quad (3.5)$$

subject to :  $\mathbf{W} \geq 0$ ,  $\mathbf{W}^T = \mathbf{W}$ ,  $\|\mathbf{W}\|_F^2 = 1$ ,

$\forall n$ ,  $\sum_{h \in \mathcal{H}_n} \alpha_{n,h} = 1$ ,  $\sum_{m \in \mathcal{M}_n} \beta_{n,m} = 1$ , and  $\alpha_{n,h} \geq 0$ ,  $\beta_{n,m} \geq 0$ ,

121 where  $E_{miss}(z_n) = -\sum_{m \in \mathcal{M}_n} \beta_{n,m} \log \beta_{n,m}$ ,  $E_{hit}(z_n) = -\sum_{h \in \mathcal{H}_n} \alpha_{n,h} \log \alpha_{n,h}$ , and  $\sigma$  is a hyperparameter  
 122 that can be tuned via internal cross-validation.

123 We also design the following optimization procedure containing two iterative steps to find  $\mathbf{W}$  that  
 124 minimizes the cost function. The framework starts from a randomly initialized  $\mathbf{W}$  and stops when the  
 125 change of cost function is less than a preset limit or the iteration number reaches a preset threshold. In  
 126 practice, we find that it typically takes ten times to stop and obtain good results. And based on our  
 127 experiments, the different initialization of  $\mathbf{W}$  will not influence the results of the iterative optimization.  
 128 Our iterative optimization strategy is efficient to achieve reasonably good results. The computation  
 129 time of IMMIGRATE is comparable to other interaction related methods such as SODA [12], hierNet  
 130 [13].

131 The visualization of optimization procedure is in Figure. 1, where  $\Delta C$  is the change of cost function  
 132 Eq. 3.5 in one iteration and  $\epsilon$  is a pre-set limit.

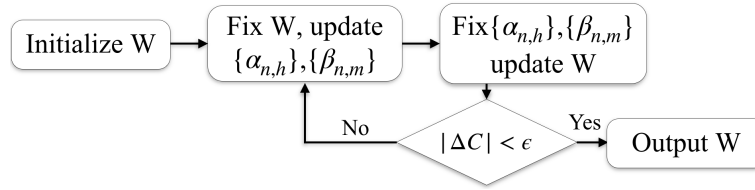


Figure 1. Flow chart of IMMIGRATE

133 Step 1: The optimization of cost function Eq. 3.5 starts from a randomly initialized  $\mathbf{W}$  (satisfying  
 134  $\mathbf{W} \geq 0$ ,  $\mathbf{W}^T = \mathbf{W}$  and  $\|\mathbf{W}\|_F^2 = 1$ ). Then the following two steps are iterated to minimize the cost  
 135 function. Step 2: Fix  $\mathbf{W}$ , update  $\{\alpha_{n,h}\}$  and  $\{\beta_{n,m}\}$ . Step 3: Fix  $\{\alpha_{n,h}\}$  and  $\{\beta_{n,m}\}$ , update  $\mathbf{W}$ .

### 136 3.4.1. Fix $\mathbf{W}$ , Update $\{\alpha_{n,h}\}$ and $\{\beta_{n,m}\}$

137 Fixing  $\mathbf{W}$  and setting  $\frac{\partial C}{\partial \alpha_{n,h}} = 0$  and  $\frac{\partial C}{\partial \beta_{n,m}} = 0$ , we can obtain the closed-form updates of  $\alpha_{n,h}$  and  
 138  $\beta_{n,m}$  as

$$\begin{aligned} \alpha_{n,h} &= \frac{\exp(-q(\vec{x}_n, \vec{x}_h)/\sigma)}{\sum_{h \in \mathcal{H}_n} \exp(-q(\vec{x}_n, \vec{x}_h)/\sigma)}, \\ \beta_{n,m} &= \frac{\exp(-q(\vec{x}_n, \vec{x}_m)/\sigma)}{\sum_{k \in \mathcal{M}_n} \exp(-q(\vec{x}_n, \vec{x}_k)/\sigma)}. \end{aligned} \quad (3.6)$$

The Hessian matrix of  $C$  w.r.t. probability pair  $(\alpha_{n,h}, \beta_{n,m})$  is:

$$\frac{\partial^2 C}{\partial(\alpha_{n,h}, \beta_{n,m})} = \begin{pmatrix} \sigma/\alpha_{n,h} & \partial^2 C / \partial \beta_{n,m} \alpha_{n,h} \\ \partial^2 C / \partial \beta_{n,m} \alpha_{n,h} & -\sigma/\beta_{n,m} \end{pmatrix}. \quad (3.7)$$

139 Since  $\alpha_{n,h}, \beta_{n,m} > 0$ , the determinant of the Hessian matrix is negative, where a saddle point  
 140 is found in  $(\alpha_{n,h}, \beta_{n,m})$  space. Therefore, the cost function  $C$  achieves its local minimum and local  
 141 maximum w.r.t.  $\alpha_{n,h}$  and  $\beta_{n,m}$ , respectively.

### 142 3.4.2. Fix $\{\alpha_{n,h}\}$ and $\{\beta_{n,m}\}$ , Update $\mathbf{W}$

143 Fixing  $\alpha_{n,h}$  and  $\beta_{n,m}$ , the minimization w.r.t.  $\mathbf{W}$  is convex. In Eq. 3.5,  $\mathbf{W}$  satisfies  $\mathbf{W} \geq 0$ ,  $\mathbf{W}^T =$   
 144  $\mathbf{W}$ ,  $\|\mathbf{W}\|_F^2 = 1$ . In our iterative optimization strategy, we impose  $\mathbf{W}$  to be a distance metric for  
 145 computation. Then, a closed-form solution to  $\mathbf{W}$  can be derived (see Eq. 3.9).

**Theorem 3.1.** *With  $\{\alpha_{n,h}\}$  and  $\{\beta_{n,m}\}$  fixed, the cost function Eq. 3.5 has a closed-form solution to updating  $\mathbf{W}$ .*

$$\Sigma = \sum_{n=1}^N \Sigma_{n,H} - \Sigma_{n,M}, \quad \Sigma \psi_i = \mu_i \psi_i, \quad (3.8)$$

where  $\Sigma_{n,H} = \sum_{h \in \mathcal{H}_n} \alpha_{n,h} |\vec{x}_n - \vec{x}_h| |\vec{x}_n - \vec{x}_h|^T$ ,  $\Sigma_{n,M} = \sum_{m \in \mathcal{M}_n} \beta_{n,m} |\vec{x}_n - \vec{x}_m| |\vec{x}_n - \vec{x}_m|^T$ , and  $\|\psi_i\|_2^2 = 1$ ,  $\mu_1 \leq \mu_2 \leq \dots \leq \mu_A$ .  $\psi_i$ 's and  $\mu_i$ 's are the eigenvectors and eigenvalues of  $\Sigma$  separately.

$$\mathbf{W} = \Phi \Phi^T, \quad (3.9)$$

146 where  $\Phi = (\sqrt{\eta_1} \psi_1, \sqrt{\eta_2} \psi_2, \dots, \sqrt{\eta_A} \psi_A)$ ,  $\sqrt{\eta_i} = \sqrt{(-\mu_i)^+ / \sqrt{\sum_{i=1}^A ((-\mu_i)^+)}}$ .

**Proof.** Since  $\mathbf{W}$  is a distance metric matrix, it is symmetric and positive-semidefinite. Eigenvalue decomposition of  $\mathbf{W}$  is

$$\begin{aligned} \mathbf{W} &= P \Lambda P^T = P \Lambda^{1/2} \Lambda^{1/2} P^T, \\ &= [\sqrt{\lambda_1} p_1, \dots, \sqrt{\lambda_A} p_A] [\sqrt{\lambda_1} p_1, \dots, \sqrt{\lambda_A} p_A]^T, \end{aligned} \quad (3.10)$$

147 where  $P$  is an orthogonal matrix. Thus,  $\langle p_i, p_j \rangle = 0$ .

148 Let  $\Phi = [\phi_1, \dots, \phi_A] = [\sqrt{\lambda_1} p_1, \dots, \sqrt{\lambda_A} p_A]$ , where  $\langle \phi_i, \phi_j \rangle = 0$  and  $\lambda_1 \geq \lambda_2 \geq \dots \geq \lambda_A$ .

The constraint  $\|\mathbf{W}\|_F^2 = 1$  can be simplified since  $\mathbf{W}$  can be decomposed to be some orthogonal vectors,

$$\|\mathbf{W}\|_F^2 = \sum_{i,j} w_{i,j}^2 = \sum_i (\phi_i^T \phi_i)^2 = 1. \quad (3.11)$$

Let us rearrange the Eq. 3.5:

$$\begin{aligned} &\sum_{h \in \mathcal{H}_n} \alpha_{n,h} |\vec{x}_n - \vec{x}_h| |\vec{x}_n - \vec{x}_h|^T \mathbf{W} |\vec{x}_n - \vec{x}_h| \text{tr}(\mathbf{W} \sum_{h \in \mathcal{H}_n} \alpha_{n,h} |\vec{x}_n - \vec{x}_h| |\vec{x}_n - \vec{x}_h|^T), \\ \text{tr}(\mathbf{W} \Sigma_{n,H}) &= \text{tr}(\Sigma_{n,H} \sum_{i=1}^A \phi_i \phi_i^T) = \sum_{i=1}^A \phi_i^T \Sigma_{n,H} \phi_i. \end{aligned} \quad (3.12)$$

Then, Eq. 3.5 can be simplified as follows:

$$\begin{aligned} C &= \sum_{i=1}^A \phi_i^T \Sigma \phi_i, \\ \text{subject to : } \|\mathbf{W}\|_F^2 &= \sum_i (\phi_i^T \phi_i)^2 = 1, \langle \phi_i, \phi_j \rangle = 0, \end{aligned} \quad (3.13)$$

149 where  $\Sigma = \sum_{n=1}^N \Sigma_{n,H} - \Sigma_{n,M}$  and  $\Sigma_{n,H} = \sum_{h \in \mathcal{H}_n} \alpha_{n,h} |\vec{x}_n - \vec{x}_h| |\vec{x}_n - \vec{x}_h|^T$ ,  $\Sigma_{n,M} = \sum_{m \in \mathcal{M}_n} \beta_{n,m} |\vec{x}_n -$   
150  $\vec{x}_m| |\vec{x}_n - \vec{x}_m|^T$ .

151 The orthogonal condition will be ignored when we derive the closed-form solution because this  
152 condition has already been satisfied at the last step.

The Lagrangian of Eq. 3.13 is easy to obtain:

$$L = \sum_{i=1}^A \phi_i^T \Sigma \phi_i + \lambda \left( \sum_{i=1}^A (\phi_i^T \phi_i)^2 - 1 \right). \quad (3.14)$$

And derive  $L$  with respect to  $\phi_i$ :

$$\partial L / \partial \phi_i = 2 \Sigma \phi_i + 4 \lambda \phi_i^T \phi_i \phi_i = 0. \quad (3.15)$$

Denote  $\phi_i / \|\phi_i\|_2 := \psi_i$ . From Eq. 3.15,

$$\Sigma \psi_i = \mu_i \psi_i, \quad (3.16)$$

153 where  $\mu_i = -2\lambda \|\phi_i\|_2^2$ .  $\psi_i$  and  $\mu_i$  are the eigenvector and eigenvalue of  $\Sigma$ , separately.

154 Let  $\phi_i = \sqrt{\eta_i}\psi_i$ ,  $\eta_i \geq 0$ . Thus,  $C = \sum_{i=1}^A \sqrt{\eta_i}\psi_i^T \Sigma \sqrt{\eta_i}\psi_i = \sum_{i=1}^A \eta_i \mu_i \psi_i^T \psi_i = \sum_{i=1}^A \eta_i \mu_i$ , and  
 155  $\|\mathbf{W}\|_F^2 = \sum_i (\sqrt{\eta_i}\psi_i^T \sqrt{\eta_i}\psi_i)^2 = \sum_i (\eta_i)^2 = 1$ .  
 Then, Eq. 3.13 can be simplified to be

$$C = \sum_{i=1}^A \eta_i \mu_i, \text{ subject to : } \sum_{i=1}^A (\eta_i)^2 = 1, \eta_i \geq 0. \quad (3.17)$$

It is excited to notice Eq. 3.17 is exactly the same as the original Relief Algorithm (Algorithm 1):

$$\vec{\eta} = (-\vec{\mu})^+ / \|(-\vec{\mu})^+\|_2, \quad (3.18)$$

156 where  $(\vec{a})^+ = [\max(a_1, 0), \max(a_2, 0), \dots, \max(a_I, 0)]$ , and  $\phi_i = \sqrt{\eta_i}\psi_i$ .

Using  $\Phi = [\phi_1, \dots, \phi_A] = [\sqrt{\lambda_1}p_1, \dots, \sqrt{\lambda_A}p_A]$ ,

$$\mathbf{W} = \Phi\Phi^T. \quad (3.19)$$

157 The orthogonal condition is achieved, because  $\|\mathbf{W}\|_F^2 = \sum_i (\phi_i^T \phi_i)^2 = 1$ .

158 In addition, since  $\mathbf{W} = \Phi\Phi^T$ , updated  $\mathbf{W}$  is also a distance metric.  $\square$

---

### Algorithm 2 IMMIGRATE Algorithm

---

**Input:** a training dataset  $\{z_n = (\vec{x}_n, y_n)\}_{n=1, \dots, N}$ .

**Initialization:** Let  $t = 0$ , randomly initialize  $\mathbf{W}^{(0)}$  satisfying  $\mathbf{W}^{(0)} \geq 0$ ,  $\mathbf{W}^T = \mathbf{W}$ ,  $\|\mathbf{W}^{(0)}\|_F^2 = 1$ .

**repeat**

    Calculate  $\{\alpha_{n,h}^{(t+1)}\}$ ,  $\{\beta_{n,m}^{(t+1)}\}$  with Eq. 3.6.

    Calculate  $\mathbf{W}^{(t+1)}$  with Theorem 3.1, Eq. 3.9.

$t = t+1$ .

**until** the change of C in Eq. 3.5 is small enough or the iteration indicator  $t$  reaches a preset limit.

**Output:**  $\mathbf{W}^{(t)}$ .

---

#### 159 3.4.3. Weight Pruning

160 The previous Relief-based algorithms offer options to remove weights lower than a preset  
 161 threshold. IMMIGRATE offers a similar option to prune small weights: set small elements in  $\mathbf{W}$   
 162 to 0. By default, we use a threshold to prune small weights to 0, where  $\mathbf{W}$  should be normalized w.r.t.  
 163 Frobenius norm after the pruning.

#### 164 3.4.4. Predict New Samples

We design a new prediction method using the learned weight matrix  $\mathbf{W}$ :

$$\hat{y}' = \arg \min_c \sum_{y_n=c} \alpha_n^c(\vec{x}') q(\vec{x}', \vec{x}_n), \quad (3.20)$$

$$\alpha_n^c(\vec{x}') = \frac{\exp(-q(\vec{x}', \vec{x}_n)/\sigma)}{\sum_{y_k=c} \exp(-q(\vec{x}', \vec{x}_k)/\sigma)},$$

165 where  $z' = (\vec{x}', y')$  is a new instance,  $c$  denotes the class and  $\hat{y}'$  is the predicted label. This prediction  
 166 method assigns a new instance to a class that maximizes its hypothesis-margin using the learned  
 167 weight matrix  $\mathbf{W}$ , which makes it more reasonable than the  $k$ -NN method used in the traditional  
 168 Relief-based algorithms.

### 169 3.5. IMMIGRATE in Ensemble Learning

170 Boosting [10,14,15] has been widely used to create ensemble learners that produce the  
 171 state-of-the-art results in many tasks. Boosting combines a set of relatively weak base learners to create  
 172 a much stronger learner. To use IMMIGRATE as the base classifier in the AdaBoost algorithm [14],  
 173 we modify the cost function Eq. 3.5 to include sample weights and use the modified version in the  
 174 boosting iterations. We name the algorithm BIM, standing for **B**oosted **I**MMIGRATE (Refer to Eq. 3.21  
 175 and Algorithm 3 for the details of BIM. BIM schedules the adjustment of the hyperparameter  $\sigma$  in  
 176 its boosting iterations. It starts with letting  $\sigma$  be a predefined  $\sigma_{max}$  and gradually decreases  $\sigma_{max}$  by  
 177  $(\sigma_{min}/\sigma_{max})^{1/T}$  in each interaction until reaching  $\sigma_{min}$ , where  $T$  is a predefined maximum number of  
 178 boosting iterations.

$$\begin{aligned}
 C &= \sum_{n=1}^N D(\vec{x}_n) \left( \sum_{h \in \mathcal{H}_n} \alpha_{n,h} |\vec{x}_n - \vec{x}_h|^T \mathbf{W} |\vec{x}_n - \vec{x}_h| - \sum_{m \in \mathcal{M}_n} \beta_{n,m} |\vec{x}_n - \vec{x}_m|^T \mathbf{W} |\vec{x}_n - \vec{x}_m| \right) \\
 &+ \sigma \sum_{n=1}^N D(\vec{x}_n) [E_{miss}(z_n) - E_{hit}(z_n)], \tag{3.21} \\
 &\text{subject to : } \mathbf{W} \geq 0, \mathbf{W}^T = \mathbf{W}, \|\mathbf{W}\|_F^2 = 1, \\
 &\forall n, \sum_{h \in \mathcal{H}_n} \alpha_{n,h} = 1, \sum_{m \in \mathcal{M}_n} \beta_{n,m} = 1, \text{ and } \alpha_{n,h} \geq 0, \beta_{n,m} \geq 0,
 \end{aligned}$$

179 where  $E_{miss}(z_n) = -\sum_{m \in \mathcal{M}_n} \beta_{n,m} \log \beta_{n,m}$ ,  $E_{hit}(z_n) = -\sum_{h \in \mathcal{H}_n} \alpha_{n,h} \log \alpha_{n,h}$ ,  $\sum_{n=1}^N D(\vec{x}_n) = 1$ , and  
 180  $D(\vec{x}_n) \geq 0, \forall n$

---

#### Algorithm 3 BIM Algorithm

---

$T$ : the number of classifiers for BIM.

**Input** : a training dataset  $\{z_n = (\vec{x}_n, y_n)\}_{n=1, \dots, N}$ .

**Initialization** : for each  $\vec{x}_n$ , set  $D_1(\vec{x}_n) = 1/N$ .

**for**  $t := 1$  **to**  $T$  **do**

Limit max number of iteration of IMMIGRATE less than preset.

Train weak IMMIGRATE classifier  $h_t(x)$  using a chosen  $\sigma_t$  and weights  $D_t(x)$  by Eq. 3.21.

Compute the error rate  $\epsilon_t$  as  $\epsilon_t = \sum_{i=1}^N D_t(x_i) I[y_i \neq h_t(x_i)]$ .

**if**  $\epsilon_t \geq 1/2$  or  $\epsilon_t = 0$  **then**

Discard  $h_t$ ,  $T = T - 1$  and continue .

Set  $\alpha_t = 0.5 \times \log[(1 - \epsilon_t)/\epsilon_t]$ .

Update  $D(x_i)$ : For each  $x_i$ ,

$$D_{t+1}(x_i) = D_t(x_i) \exp(\alpha_t I[y_i \neq h_t(x_i)]).$$

Normalize  $D_{t+1}(x_i)$ , so that  $\sum_{i=1}^N D_{t+1}(x_i) = 1$ .

**Output**:  $h_{final}(x) = \arg \max_{y \in \{0,1\}} \sum_{t: h_t(x)=y} \alpha_t$ .

---

### 181 3.6. IMMIGRATE for High-Dimensional Data Space

182 When applied to high-dimensional data, IMMIGRATE can incur a high computational cost  
 183 because it considers the interactions between every feature pair. To reduce the computational cost, we  
 184 first use IM4E [8] to learn a feature weight vector, which is used to initialize the diagonal elements  
 185 of  $\mathbf{W}$  in the proposed quadratic-Manhattan measurement. We also use the learned feature weight  
 186 vector to choose the features with weights above a preset limit. In the rest computation, we only model  
 187 the interactions between those chosen features. The remaining features are empirically decided  
 188 and can be adjusted accordingly to the need of a specific application. We term this procedure  
 189 IM4E-IMMIGRATE, which is a sub-optimal solution but effective and efficient. It can also be boosted  
 190 (Boosted IM4E-IMMIGRATE) to be stronger.



## 191 4. Experiments

192 In our experiments, all continuous features are normalized with mean zero and unit  
 193 variance. And cross-validation is used here to compare the performances of various approaches.  
 194 We have implemented IMMIGRATE in R and MATLAB. The R package is available at  
 195 <https://CRAN.R-project.org/package=Immigrate>, and the MATLAB version is available at  
 196 <https://github.com/RuzhangZhao/Immigrate-MATLAB> is also available. Both IMMIGRATE and  
 197 BIM can be accelerated by parallel computing as their computations are matrix-based.

### 198 4.1. Synthetic Dataset

199 We first test the robustness of the IMMIGRATE algorithm using a synthesized dataset where  
 200 we have two interacting features following Gaussian distributions in a binary classification setting.  
 201 The simulated dataset contains 100 samples from one class governed by a Gaussian distribution with  
 202 mean  $(4, 2)^T$  and variance  $\begin{pmatrix} 1 & 0.5 \\ 0.5 & 1 \end{pmatrix}$  and another 100 samples from the other class governed by a  
 203 Gaussian distribution with mean  $(6, 0)^T$  and the same variance. In addition, we add noise following  
 204 a Gaussian distribution with mean  $(8, -2)^T$  and variance  $\begin{pmatrix} 8 & 4 \\ 4 & 8 \end{pmatrix}$  to the first class, and add noises  
 205 following a Gaussian distribution with mean  $(2, 4)^T$  and the same variance to the second class. Fig. 2  
 206 shows a scatter plot of the synthesized dataset containing 10% samples from the noise distributions.  
 207 The slope of the orange dotted line in Fig. 2 is 1, which separates data with different labels.

208 The noises are included to disturb the detection of the interaction term. The noise level starts from  
 209 5%, and gradually increases by 5% to 50%. As the baseline, we apply logistic regression and see that  
 210 the  $t$ -test  $p$ -values of the interaction coefficients increase from  $3 \times 10^{-11}$ ,  $7 \times 10^{-5}$ , to 0.7 when the noise  
 211 levels increase from 0, 10%, to 50%. Local Feature Extraction (LFE, Sun and Wu [7]) is a Relief-based  
 212 algorithm which considers interaction terms indirectly, though the interaction information is only used  
 213 for feature extraction. We run IMMIGRATE and LFE on the synthesized datasets and compare the  
 214 weights of the interaction term between features 1 and 2 in Fig. 3, which shows IMMIGRATE is more  
 215 robust than LFE.

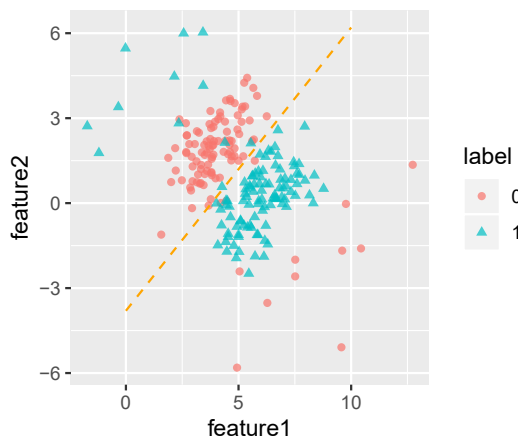


**Figure 2.** The synthetic dataset with 10% noise.

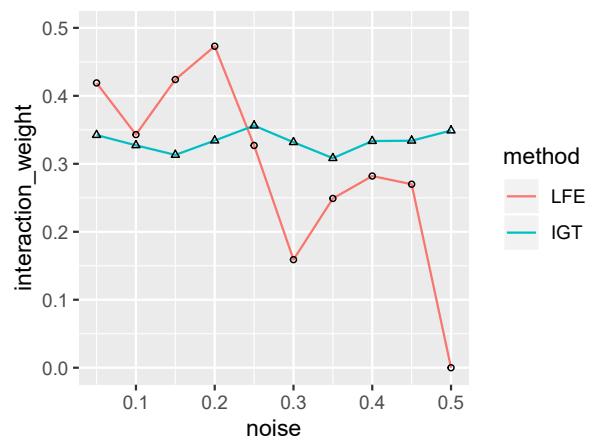


**Figure 3.** IMMIGRATE (IGT) is more robust than LFE.

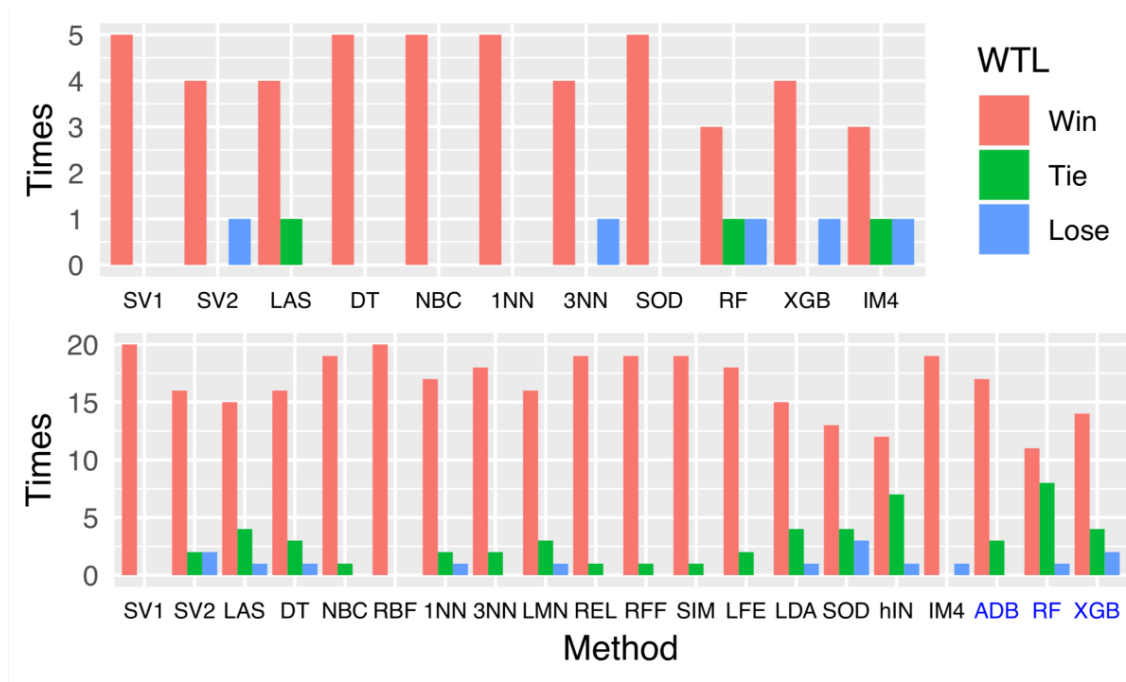


**Figure 4.** Results of paired *t*-test on gene expression datasets (top subplot) and UCI datasets (bottom subplot). The top plot shows how well (i.e., "Win" (red bars), "Tie" (green bars), and "Lose" (blue bars)) our Boosted IM4E-IMMIGRATE performs compared with other approaches. In the bottom plot, the results of methods labeled in black are the comparisons with our IMMIGRATE, and the results of methods (ABD, RF, and XGB) labeled in blue are the comparisons with our BIM.

#### 216 4.2. Real Datasets

217 We compare IMMIGRATE with several existing popular methods using real datasets from the UCI  
 218 database. The following existing algorithms are used in the comparison: Support Vector Machine [16]  
 219 with Sigmoid Kernel (SV1), Support Vector Machine with Radial basis function Kernel (SV2), LASSO  
 220 (LAS) [17], Decision Tree (DT) [15], Naive Bayes Classifier (NBC) [18], Radial basis function Network  
 221 (RBF) [19], 1-Nearest Neighbor (1NN) [20], 3-Nearest Neighbor (3NN), Large Margin Nearest Neighbor  
 222 (LMN) [21], Relief (REL) [2], ReliefF (RFF) [4,22], Simba (SIM) [3], and Linear Discriminant Analysis  
 223 (LDA) [23]. In addition, several methods designed for detecting interaction terms are included: LFE [7],  
 224 Stepwise conditional likelihood variable selection for Discriminant Analysis (SOD) [12], and hierNet  
 225 (hIN) [13]. We also include three most widely used and competitive ensemble learners: Adaptive  
 226 Boosting (ADB) [14,15], Random Forest (RF) [24], and XgBoost (XGB) [25]. We use the following  
 227 abbreviations when presenting the results: IM4 for IM4E, IGT for IMMIGRATE, and B4G for the  
 228 boosted IM4E-IMMIGRATE.

229 Whenever possible, we use the settings of the above methods reported in their original papers:  
 230 LMNN uses 3-NN classifier; Relief and Simba use Euclidean distance and 1-NN classifier; ReliefF  
 231 uses Manhattan distance and  $k$ -NN classifier ( $k=1,3,5$  is decided by internal cross-validation); in  
 232 SODA,  $\text{gam} (=0,0.5,1)$  is determined by internal cross-validation and logistic regression is used for  
 233 prediction. The IM4E algorithm owns two hyperparameters  $\lambda$  and  $\sigma$ . We fix  $\lambda = 1$  as it has no actual  
 234 contribution and tune  $\sigma$  as suggested by Bei and Hong [8]. Hence, the IMMIGRATE algorithm only  
 235 has one hyperparameter  $\sigma$ . When tuning  $\sigma$ , we gradually decrease  $\sigma$  from  $\sigma_0 = 4$  by half each time  
 236 until it is not larger than 0.2. The preset limit for weight pruning is  $1/A$ , where  $A$  is the number  
 237 of features. Also, the preset iteration number is chosen to be 10. For each dataset,  $\sigma$  and whether  
 238 weight pruning is applied are determined by the best internal cross-validation results. For BIM, we  
 239 use  $\sigma_{max} = 4$ ,  $\sigma_{min} = 0.2$ , and the maximal number of boosting iterations  $T$  is 100. The preset threshold  
 240 in IM4E-IMMIGRATE is  $2/A$ .

241 We repeat ten-fold cross-validation ten times for each algorithm on each dataset, i.e., 100 trials  
 242 are carried out. When comparing two algorithms (i.e., A vs B), we calculate the paired Student's  
 243 *t*-test using the results of 100 trials. First, the null hypothesis is there is no difference between the  
 244 performances of A and those of B. When the *p*-value is larger than the significant level cutoff 0.05, we  
 245 say A "Tie" B, which means there is no significant difference between their performances. When the  
 246 *p*-value is smaller than the significant level cutoff 0.05, the second null hypothesis is the performances  
 247 of B are no worse than those of A. When the new *p*-value is smaller than the significant level cutoff 0.05,  
 248 we say A "Win" B which means A on average performs better than B on this dataset (i.e., A performs  
 249 significantly better than B), and vice versa.

#### 250 4.2.1. Gene Expression Datasets

251 Gene expression datasets typically have thousands of features. We use the following five gene  
 252 expression datasets for feature selections: GLI [26], Colon [27](COL), Myeloma (ELO) [28], Breast (BRE)  
 253 [29], Prostate (PRO) [30]. All datasets have more than 10,000 features. Refer to Table A1 in Appendix A  
 254 for details of all datasets.

255 We perform ten-fold cross-validation ten times, i.e., 100 trials in total. The results are summarized  
 256 in Table 1. The last row "(W,T,L)" indicates the number of times that the Boosted IM4E-IMMIGRATE  
 257 (B4G) W,T,L (win,tie,loss) compared with each algorithm by the paired Student's *t*-test with the  
 258 significance level of  $\alpha = 0.05$ . The comparison results are also summarized in Figure 4 (top plot) for  
 259 easy comparison. Although our B4G is not always the best, it outperforms other methods in most cases.  
 260 In particular, when IM4E-IMMIGRATE (EGT) is compared with other methods, it also outperforms in  
 261 most cases.

**Table 1.** Summarizes the accuracies on five high-dimensional gene expression datasets.

Data	SV1	SV2	LAS	DT	NBC	1NN	3NN	SOD	RF	XGB	IM4	EGT	B4G
GLI	85.1	86.0	85.2	83.8	83.0	88.7	87.7	88.7	87.6	86.3	87.5	89.1	89.9
COL	73.7	82.0	80.6	69.2	71.1	72.1	77.9	78.1	82.6	79.5	84.3	78.6	82.5
ELO	72.9	90.2	74.6	77.3	76.3	85.6	91.3	86.9	79.2	77.9	88.9	88.6	88.4
BRE	76.0	88.7	91.4	76.4	69.4	83.0	73.6	82.6	86.3	87.3	88.1	90.2	91.5
PRO	71.3	69.9	87.9	86.4	68.0	83.2	82.7	83.2	91.8	90.5	88.0	89.5	89.7
W,T,L <sup>1</sup>	5,0,0	4,0,1	4,1,0	5,0,0	5,0,0	5,0,0	4,0,1	5,0,0	3,1,1	4,0,1	3,1,1	-,-,-	-,-,-

<sup>1</sup> The last row shows the number of times Boosted IM4E-IMMIGRATE(B4G) W,T,L (win,tie,loss) compared with each algorithm by paired *t*-test

\*\* Ten-fold cross-validation is performed for ten times, namely 100 trials are carried out for each dataset. The average accuracies are reported on the corresponding datasets in Table 1,2,3. Here, with 100 trials and two algorithms A and B, paired Student's *t*-test is carried out between the results of these two algorithms. Under the significance level of  $\alpha = 0.05$ , algorithm A is significantly better than (i.e. win) another algorithm B on a dataset if the *p*-value of the paired Student's *t*-test with corresponding null hypothesis is less than  $\alpha = 0.05$ . (The rule also applies to experiments on UCI datasets) .

#### 262 4.2.2. UCI Datasets

263 We also carry out an extensive comparison using many UCI datasets [31]: BCW, CRY, CUS, ECO,  
 264 GLA, HMS, IMM, ION, LYM, MON, PAR, PID, SMR, STA, URB, USE and WIN. Refer to Appendix A  
 265 Table A1 for the full names and links for those datasets. If a dataset has more than two classes, we use  
 266 two classes with the largest sample size. In addition, we use three large-scale datasets: CRO\*, ELE\*,  
 267 WAV\*.

268 We perform ten-fold cross-validation ten times. Tables 2 for IMMIGRATE and Table 3 for BIM  
 269 show the average accuracies on the corresponding datasets. In Table 2, the last row "(W,T,L)" indicates  
 270 the number of times IMMIGRATE (IGT) and BIM W,T,L (win,tie,loss) when compared with each  
 271 algorithm separately by using the paired Student's *t*-test with the significance level of  $\alpha = 0.05$ . The

comparison results are also summarized in Figure 4 (bottom subplot), where the first 17 items (black) indicate the results for IMMIGRATE while the last three items (blue) indicate the results for BIM.

Although IMMIGRATE or BIM is not always the best, they outperform other methods significantly in one-to-one comparisons in terms of cross-validation results. Figure 4 (bottom subplot, black part) and Table 2 show that IMMIGRATE achieves the state-of-the-art performance as the base classifier while Figure 4 (bottom subplot, blue part) and Table 3 show BIM achieves the state-of-the-art performance as the boosted version. To visualize the feature selection results of our approaches, we plot the feature weight heat maps of four datasets (GLA, LYM, SMR and STA) in Appendix B Figure A5.

**Table 2.** Summarizes the accuracies on UCI datasets.

Data	SV1	SV2	LAS	DT	NBC	RBF	1NN	3NN	LMN	REL	RFF	SIM	LFE	LDA	SOD	hIN	IM4	IGT
BCW	61.4	66.6	71.4	70.5	62.4	56.9	68.2	72.2	69.5	66.4	67.1	67.7	67.1	73.9	65.2	71.8	66.4	74.5
CRY	72.9	90.6	87.4	85.3	84.4	89.7	89.1	85.4	87.8	73.8	77.2	79.7	86.0	88.6	86.0	87.9	86.2	89.8
CUS	86.5	88.9	89.6	89.6	89.5	86.8	86.5	88.7	88.8	82.1	84.7	84.3	86.4	90.3	90.8	90.3	87.5	90.1
ECO	92.9	96.9	98.6	98.6	97.8	94.6	96.0	97.8	97.8	89.0	90.7	91.2	93.1	99.0	97.9	98.7	97.5	98.2
GLA	64.2	76.7	72.3	79.4	69.5	73.0	81.1	78.1	79.4	64.1	63.5	67.1	81.2	72.0	75.3	75.0	78.0	87.5
HMS	63.8	64.5	67.7	72.5	67.2	66.8	66.0	69.3	71.2	65.3	66.0	65.7	64.9	69.0	67.4	69.4	66.6	69.2
IMM	74.3	70.6	74.4	84.1	77.9	67.3	69.4	77.9	76.7	69.9	71.8	69.0	75.0	75.2	72.3	70.2	80.7	83.8
ION	80.5	93.5	83.6	87.4	89.4	79.9	86.7	84.1	84.5	85.8	86.2	84.2	91.0	83.3	90.3	92.6	88.3	92.9
LYM	83.6	81.5	85.2	75.2	83.6	71.1	77.2	82.8	86.6	64.9	71.0	70.4	79.6	85.2	79.3	84.8	83.3	87.2
MON	74.4	91.7	75.0	86.4	74.0	68.2	75.1	84.4	84.9	61.4	61.8	65.0	64.8	74.4	91.9	97.2	75.6	99.5
PAR	72.7	72.5	77.1	84.8	74.1	71.5	94.6	91.4	91.8	87.3	90.3	84.6	94.0	85.6	88.2	89.5	83.2	93.8
PID	65.6	73.1	74.7	74.3	71.2	70.3	70.3	73.5	74.0	64.8	68.0	67.0	67.8	74.5	75.7	74.1	72.1	74.7
SMR	73.5	83.9	73.6	72.3	70.3	67.1	86.9	84.7	86.1	69.5	78.3	81.0	84.3	73.1	70.5	83.0	76.4	86.5
STA	69.8	71.6	70.8	68.9	71.0	69.5	67.8	70.8	71.3	59.7	64.0	63.0	66.7	71.3	71.8	69.2	70.8	75.9
URB	85.2	87.9	88.1	82.6	85.8	75.3	87.2	87.5	87.9	81.9	83.2	73.0	87.9	73.0	87.9	88.3	87.4	89.9
USE	95.7	95.2	97.2	93.2	90.6	84.9	90.5	91.5	92.0	54.5	63.7	69.5	85.8	96.9	96.2	96.5	94.1	96.4
WIN	98.3	99.3	98.6	93.1	97.3	97.2	96.4	96.6	96.5	87.2	95.0	95.0	93.8	99.7	92.9	98.9	98.2	99.0
CRO*	75.4	97.5	89.9	91.0	88.8	75.4	98.4	98.5	98.6	98.5	98.7	95.1	98.6	89.1	95.2	95.5	81.9	98.2
ELE*	72.3	95.7	79.9	80.0	82.5	70.8	81.1	83.9	89.7	64.6	75.4	76.2	79.8	79.9	93.7	93.6	83.2	93.7
WAV*	90.0	91.9	92.2	86.2	91.4	84.0	86.5	88.3	88.8	77.6	80.0	83.6	84.7	91.8	92.0	92.1	91.1	92.4
W,T,L <sup>1</sup>	20,0,0	16,2,2	15,4,1	16,3,1	19,1,0	20,0,0	17,2,1	18,2,0	16,3,1	19,1,0	19,1,0	19,1,0	18,2,0	15,4,1	13,4,3	12,7,1	19,0,1	-,-,-

<sup>1</sup> The last row (W,T,L) shows the number of times that IMMIGRATE (IGT) wins/ties/losses an existing algorithm according to the paired *t*-test on the cross-validation results.

**Table 3.** Summarizes the accuracies on UCI datasets.

Data	ADB	RF	XGB	<b>BIM</b>
BCW	78.2	78.6	78.6	78.3
CRY	90.4	92.9	89.9	91.5
CUS	90.8	91.1	91.4	91.0
ECO	98.0	98.9	98.2	98.6
GLA	85.0	87.0	87.9	86.8
HMS	65.8	72.1	70.0	72.0
IMM	77.2	84.2	81.7	86.1
ION	92.1	93.5	92.5	93.1
LYM	84.8	87.0	87.4	88.1
MON	98.4	95.8	99.1	99.7
PAR	90.5	91.0	91.9	93.2
PID	73.5	76.0	75.1	76.2
SMR	81.4	82.8	83.3	86.6
STA	69.0	71.3	69.5	74.1
URB	87.9	88.6	88.8	91.4
USE	96.0	95.3	94.9	96.1
WIN	97.5	99.1	98.2	99.1
CRO*	97.3	97.4	98.5	98.6
ELE*	91.1	92.3	95.2	94.1
WAV*	89.5	91.2	90.8	93.3
W,T,L <sup>1</sup>	<b>17,3,0</b>	<b>11,8,1</b>	<b>14,4,2</b>	<b>---</b>

<sup>1</sup> The last row (W,T,L) shows the number of times that the Boosted IMMIGRATE (**BIM**) wins/ties/losses an existing algorithm according to the paired *t*-test on the cross-validation results.

## 280 5. Related Works

281 In many recent researches, Relief-based algorithms and feature selection with interaction terms  
 282 have been well explored. Some methods are reviewed here to show the connection and differences with  
 283 our approach. The hypothesis-margin definition in Eq. 3.2 adopted in this work is also used in previous  
 284 studies, such as Bei and Hong [8]. However, Bei and Hong [8] do not consider the interactions between  
 285 features. Our work provides a measurable way to show the influence of each feature interaction.

286 Sun and Wu [7] propose local feature extraction (LFE) method which learns linear combination of  
 287 features for feature extraction. LFE explores the information of feature interaction terms indirectly,  
 288 which is partly our aim. However, LFE does not consider global information or margin stability, which  
 289 results in significant differences in the cost function and the optimization procedures.

290 Our quadratic-Manhattan measurement Eq. 3.3 is related to the Mahalanobis metric used in  
 291 previous works on metric learning, such as Large Margin Nearest Neighbor (LMNN) [21]. Weinberger  
 292 and Saul [21] use semi-definite programming for learning distance metric in LMNN. LMNN and our  
 293 approach are both based on K-Nearest Neighbor. A major difference is that our quadratic-Manhattan  
 294 measurement has matrix  $\mathbf{W}$  be a non-negative symmetric matrix (element-wise non-negative) and  
 295 its Frobenius norm  $\|\mathbf{W}\|_F = 1$ . While in metric learning, metric learning imposes the matrix to  
 296 be symmetric semi-positive definite. Actually, non-negative requirement provides IMMIGRATE  
 297 high interpretability, where items in matrix serve as interaction importance. Quadratic-Manhattan  
 298 measurement serves well in the classification task and offers a great explanation about how features,  
 299 in particular, feature interaction terms, contribute to the classification results.

## 300 6. Conclusion & Discussion

301 In this paper, a novel feature selection algorithm IMMIGRATE is proposed for detecting  
 302 and weighting interaction terms. We also develop its extended versions, such as, Boosted  
 303 IMMIGRATE (BIM) and IM4E-IMMIGRATE. A new quadratic-Manhattan measurement is proposed  
 304 to extend the hypothesis-margin. IMMIGRATE and its variants follow the principle of maximizing  
 305 stable hypothesis-margin. An iterative optimization framework is designed for implementing the  
 306 IMMIGRATE algorithm and the closed-form update of parameters is derived in Theorem 3.1. Extensive  
 307 experiments show that IMMIGRATE outperforms existing methods and improves the state-of-the-art.  
 308 BIM outperforms other boosting-based approaches. Its robustness is clearly demonstrated on  
 309 synthetic dataset where we know the ground truth. In conclusion, compared with other Relief-based  
 310 algorithms, IMMIGRATE mainly has the following advantages: (1) both local and global information  
 311 are considered; (2) interaction terms are used; (3) robust and less prone to noise; (4) easily boosted. The  
 312 computation time of IMMIGRATE variants is comparable to other methods able to detect interaction  
 313 terms.

314 There are several directions for improving IMMIGRATE. First, in section 3.4.3, small weights  
 315 are removed to obtain sparse solutions. We can explore using  $l_0$  or  $l_1$  to cut insignificant weights.  
 316 Second, to further improve the computational efficiency of IMMIGRATE for large-scale datasets, we  
 317 can improve training by using well selected prototypes [32]. Third, IMMIGRATE only considers  
 318 pair-wise interactions between features. Interactions among multiple features can play important roles  
 319 in real applications. Our work provides a basis for developing new algorithms to detect multi-feature  
 320 interactions. For example, people can use tensor form to consider weights for multi-feature interactions.  
 321 Fourth, although our iterative optimization procedure is efficient, it achieves sub-optimal solutions. In  
 322 particular, procedure 3.4.1 and 3.4.2 are both sub-optimal. It remains an open challenge to develop  
 323 better optimization algorithms. Finally, the selection of an appropriate  $\sigma$  currently relies on internal  
 324 cross-validation. A better strategy may be developed by rigorously investigating the theoretical  
 325 contributions of  $\sigma$ .

326 **Author Contributions:** methodology, R.Z. and P.H.; software, R.Z.; validation, R.Z., P.H. and J.S.L.; investigation,  
 327 R.Z., P.H. and J.S.L.; resources, R.Z., P.H. and J.S.L.; data curation, R.Z. and P.H.; writing—original draft preparation,  
 328 R.Z.; writing—review and editing, R.Z., P.H. and J.S.L.; supervision, P.H. and J.S.L.; funding acquisition, P.H. and  
 329 J.S.L.

330 **Funding:** This research was supported partially by the the National Science Foundation grants DMS-1613035,  
 331 DMS-1712714, and OAC-1920147.

332 **Acknowledgments:** The authors thank Dr. Xin Xing for the valuable suggestions to improve the work. And the  
 333 authors thank Dr. Yang Li for the helpful suggestions about R codes.

334 **Conflicts of Interest:** The authors declare no conflict of interest.

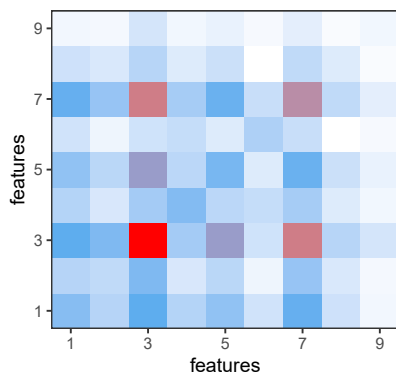
## 335 Abbreviations

336 The following abbreviations are used in this manuscript:

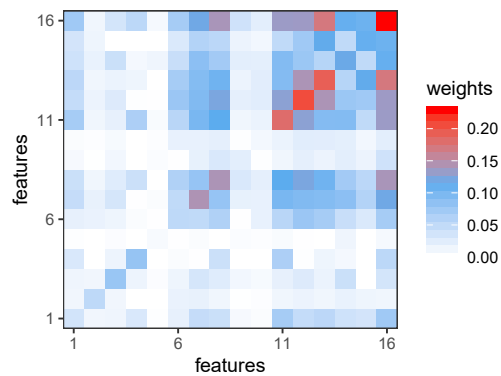
337 NH	Nearest Hit
NM	Nearest Miss
338 IM4E	Iterative Margin-Maximization under Max-Min Entropy algorithm
IMMIGRATE	<i>Iterative Max-MIn entropy marGin-maximization with inteRAction TErms</i> algorithm

339 **Appendix A Summarizes the information of Real Datasets****Table A1.** Summarizes the information of UCI datasets and gene expression datasets.

Data	No.F <sup>1</sup>	No.I <sup>2</sup>	Full Name
BCW	9	116	Breast Cancer Wisconsin (Prognostic)
CRY	6	90	Cryotherapy
CUS	7	440	Wholesale customers
ECO	5	220	Ecoli
GLA	9	146	Glass Identification
HMS	3	306	Haberman's Survival
IMM	7	90	Immunotherapy
ION	32	351	Ionosphere
LYM	16	142	Lymphograph
MON	6	432	MONK's Problems
PAR	22	194	Parkinsons
PID	8	768	Pima-Indians-Diabetes
SMR	60	208	Connectionist Bench (Sonar, Mines vs. Rocks)
STA	12	256	Statlog (Heart)
URB	147	238	Urban Land Cover
USE	5	251	User Knowledge Modeling
WIN	13	130	Wine
CRO*	28	9003	Crowdsourced Mapping
ELE*	12	10000	Electrical Grid Stability Simulated
WAV*	21	3304	Waveform Database Generator
GLI	22283	85	Gliomas Strongly Predicts Survival[26]
COL	2000	62	Tumor and Normal Colon Tissues[27]
ELO	12625	173	Myeloma[28]
BRE	24481	78	Breast Cancer[29]
PRO	12600	136	Clinical Prostate Cancer Behavior[30]

<sup>1</sup> No.F: Number of Features.<sup>2</sup> No.I: Number of Instances.340 **Appendix B Heat Maps**

GLA



LYM

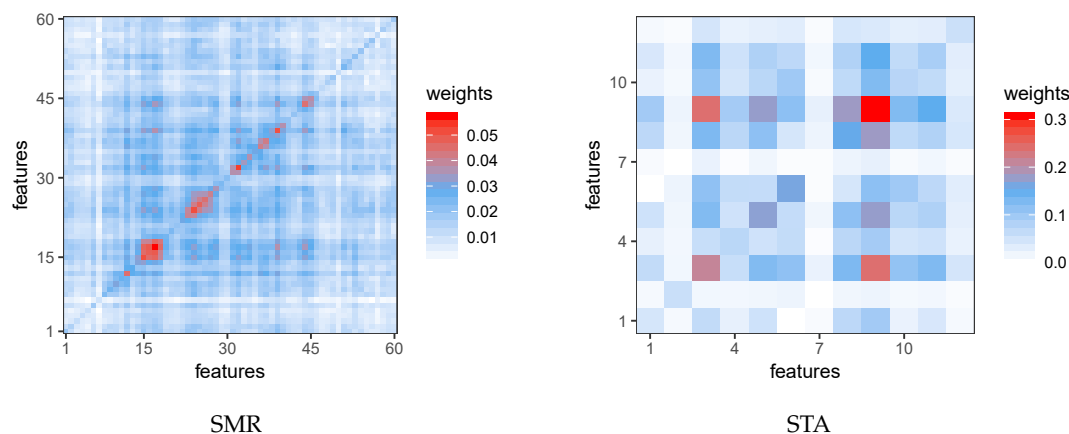


**Figure:** Heat Maps of Feature Weights Learned by IMMIGRATE.  
The color bar shows the value of corresponding colors.

## 341 References

- 342 1. Fukunaga, K. *Introduction to statistical pattern recognition*; Elsevier, 2013.
- 343 2. Kira, K.; Rendell, L.A. A practical approach to feature selection. In *Machine Learning Proceedings 1992*;  
344 Elsevier, 1992; pp. 249–256.
- 345 3. Gilad-Bachrach, R.; Navot, A.; Tishby, N. Margin based feature selection-theory and algorithms.  
346 Proceedings of the twenty-first international conference on Machine learning. ACM, 2004, p. 43.
- 347 4. Kononenko, I. Estimating attributes: analysis and extensions of RELIEF. European conference on machine  
348 learning. Springer, 1994, pp. 171–182.
- 349 5. Yang, M.; Wang, F.; Yang, P. A Novel Feature Selection Algorithm Based on Hypothesis-Margin. *JCP* **2008**,  
350 *3*, 27–34.
- 351 6. Sun, Y.; Li, J. Iterative RELIEF for feature weighting. Proceedings of the 23rd international conference on  
352 Machine learning. ACM, 2006, pp. 913–920.
- 353 7. Sun, Y.; Wu, D. A relief based feature extraction algorithm. Proceedings of the 2008 SIAM International  
354 Conference on Data Mining. SIAM, 2008, pp. 188–195.
- 355 8. Bei, Y.; Hong, P. Maximizing margin quality and quantity. Machine Learning for Signal Processing (MLSP),  
356 2015 IEEE 25th International Workshop on. IEEE, 2015, pp. 1–6.
- 357 9. Urbanowicz, R.J.; Meeker, M.; La Cava, W.; Olson, R.S.; Moore, J.H. Relief-based feature selection:  
358 introduction and review. *Journal of biomedical informatics* **2018**.
- 359 10. Schapire, R.E. The strength of weak learnability. *Machine learning* **1990**, *5*, 197–227.
- 360 11. Kuhn, H.W.; Tucker, A.W. Nonlinear programming. In *Traces and emergence of nonlinear programming*;  
361 Springer, 2014; pp. 247–258.
- 362 12. Li, Y.; Liu, J.S. Robust variable and interaction selection for logistic regression and general index models.  
363 *Journal of the American Statistical Association* **2018**, pp. 1–16.
- 364 13. Bien, J.; Taylor, J.; Tibshirani, R. A lasso for hierarchical interactions. *Annals of statistics* **2013**, *41*, 1111.
- 365 14. Freund, Y.; Schapire, R.E.; others. Experiments with a new boosting algorithm. *icml*. Citeseer, 1996, Vol. 96,  
366 pp. 148–156.
- 367 15. Freund, Y.; Mason, L. The alternating decision tree learning algorithm. *icml*, 1999, Vol. 99, pp. 124–133.
- 368 16. Soentpiet, R.; others. *Advances in kernel methods: support vector learning*; MIT press, 1999.
- 369 17. Tibshirani, R. Regression shrinkage and selection via the lasso. *Journal of the Royal Statistical Society. Series*  
370 *B (Methodological)* **1996**, pp. 267–288.
- 371 18. John, G.H.; Langley, P. Estimating continuous distributions in Bayesian classifiers. Proceedings of the  
372 Eleventh conference on Uncertainty in artificial intelligence. Morgan Kaufmann Publishers Inc., 1995, pp.  
373 338–345.
- 374 19. Haykin, S. *Neural networks: a comprehensive foundation*; Prentice Hall PTR, 1994.
- 375 20. Aha, D.W.; Kibler, D.; Albert, M.K. Instance-based learning algorithms. *Machine learning* **1991**, *6*, 37–66.



- 376 21. Weinberger, K.Q.; Saul, L.K. Distance metric learning for large margin nearest neighbor classification.  
377 *Journal of Machine Learning Research* **2009**, *10*, 207–244.
- 378 22. Robnik-Šikonja, M.; Kononenko, I. Theoretical and empirical analysis of ReliefF and RReliefF. *Machine*  
379 *learning* **2003**, *53*, 23–69.
- 380 23. Fisher, R.A. The use of multiple measurements in taxonomic problems. *Annals of eugenics* **1936**, *7*, 179–188.
- 381 24. Breiman, L. Random forests. *Machine learning* **2001**, *45*, 5–32.
- 382 25. Chen, T.; Guestrin, C. Xgboost: A scalable tree boosting system. Proceedings of the 22nd acm sigkdd  
383 international conference on knowledge discovery and data mining. ACM, 2016, pp. 785–794.
- 384 26. Freije, W.A.; Castro-Vargas, F.E.; Fang, Z.; Horvath, S.; Cloughesy, T.; Liau, L.M.; Mischel, P.S.; Nelson, S.F.  
385 Gene expression profiling of gliomas strongly predicts survival. *Cancer research* **2004**, *64*, 6503–6510.
- 386 27. Alon, U.; Barkai, N.; Notterman, D.A.; Gish, K.; Ybarra, S.; Mack, D.; Levine, A.J. Broad patterns of gene  
387 expression revealed by clustering analysis of tumor and normal colon tissues probed by oligonucleotide  
388 arrays. *Proceedings of the National Academy of Sciences* **1999**, *96*, 6745–6750.
- 389 28. Tian, E.; Zhan, F.; Walker, R.; Rasmussen, E.; Ma, Y.; Barlogie, B.; Shaughnessy Jr, J.D. The role of the  
390 Wnt-signaling antagonist DKK1 in the development of osteolytic lesions in multiple myeloma. *New*  
391 *England Journal of Medicine* **2003**, *349*, 2483–2494.
- 392 29. Van't Veer, L.J.; Dai, H.; Van De Vijver, M.J.; He, Y.D.; Hart, A.A.; Mao, M.; Peterse, H.L.; Van Der Kooy, K.;  
393 Marton, M.J.; Witteveen, A.T.; others. Gene expression profiling predicts clinical outcome of breast cancer.  
394 *nature* **2002**, *415*, 530.
- 395 30. Singh, D.; Febbo, P.G.; Ross, K.; Jackson, D.G.; Manola, J.; Ladd, C.; Tamayo, P.; Renshaw, A.A.; D'Amico,  
396 A.V.; Richie, J.P.; others. Gene expression correlates of clinical prostate cancer behavior. *Cancer cell* **2002**,  
397 *1*, 203–209.
- 398 31. Frank, A.; Asuncion, A. UCI Machine Learning Repository [<http://archive.ics.uci.edu/ml>]. Irvine, CA:  
399 University of California. *School of information and computer science* **2010**, *213*, 2–2.
- 400 32. Garcia, S.; Derrac, J.; Cano, J.; Herrera, F. Prototype selection for nearest neighbor classification: Taxonomy  
401 and empirical study. *IEEE transactions on pattern analysis and machine intelligence* **2012**, *34*, 417–435.

402 **Sample Availability:** Samples of the compounds ..... are available from the authors.

403 © 2020 by the authors. Submitted to *Entropy* for possible open access publication under the terms and conditions  
404 of the Creative Commons Attribution (CC BY) license (<http://creativecommons.org/licenses/by/4.0/>).